



TECHNICAL REPORT AMR-SS-08-09

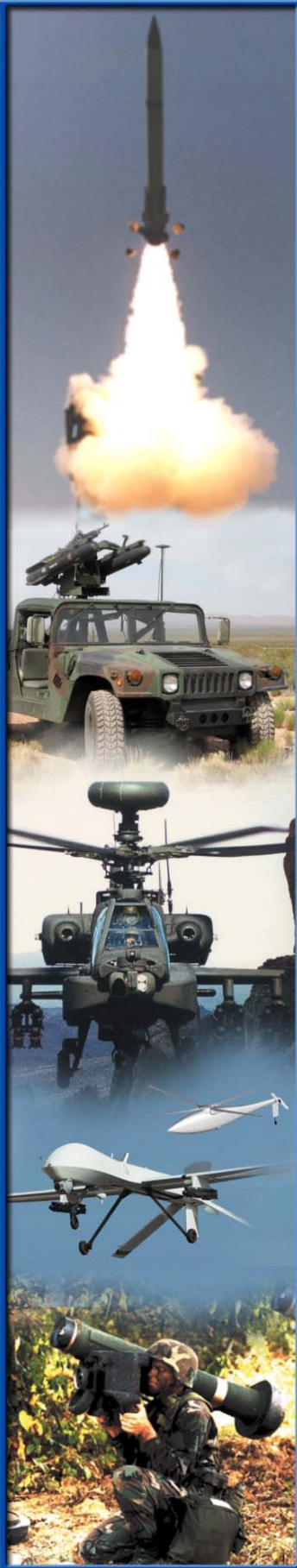
GUIDELINES FOR GRIDDING SIMPLE FLOWS — THE FLAT PLATE IN LAMINAR FLOW

Milton E. Vaughn, Jr.

System Simulation and Development Directorate
Aviation and Missile Research, Development, and
Engineering Center

January 2008

Approved for public release; distribution is unlimited.



DESTRUCTION NOTICE

FOR CLASSIFIED DOCUMENTS, FOLLOW THE PROCEDURES IN DoD 5200.22-M, INDUSTRIAL SECURITY MANUAL, SECTION II-19 OR DoD 5200.1-R, INFORMATION SECURITY PROGRAM REGULATION, CHAPTER IX. FOR UNCLASSIFIED, LIMITED DOCUMENTS, DESTROY BY ANY METHOD THAT WILL PREVENT DISCLOSURE OF CONTENTS OR RECONSTRUCTION OF THE DOCUMENT.

DISCLAIMER

THE FINDINGS IN THIS REPORT ARE NOT TO BE CONSTRUED AS AN OFFICIAL DEPARTMENT OF THE ARMY POSITION UNLESS SO DESIGNATED BY OTHER AUTHORIZED DOCUMENTS.

TRADE NAMES

USE OF TRADE NAMES OR MANUFACTURERS IN THIS REPORT DOES NOT CONSTITUTE AN OFFICIAL ENDORSEMENT OR APPROVAL OF THE USE OF SUCH COMMERCIAL HARDWARE OR SOFTWARE.

REPORT DOCUMENTATION PAGE			Form Approved OMB No. 074-0188	
Public reporting burden for this collection of information is estimated to average 1 hour per response, including the time for reviewing instructions, searching existing data sources, gathering and maintaining the data needed, and completing and reviewing this collection of information. Send comments regarding this burden estimate or any other aspect of this collection of information, including suggestions for reducing this burden to Washington Headquarters Services, Directorate for Information Operations and Reports, 1215 Jefferson Davis Highway, Suite 1204, Arlington, VA 22202-4302, and to the Office of Management and Budget, Paperwork Reduction Project (0704-0188), Washington, DC 20503				
1. AGENCY USE ONLY	2. REPORT DATE January 2008	3. REPORT TYPE AND DATES COVERED Final		
4. TITLE AND SUBTITLE Guidelines for Gridding Simple Flows — The Flat Plate in Laminar Flow			5. FUNDING NUMBERS	
6. AUTHOR(S) Milton E. Vaughn, Jr.				
7. PERFORMING ORGANIZATION NAME(S) AND ADDRESS(ES) Commander, U.S. Army Research, Development, and Engineering Command ATTN: AMSRD-AMR-SS-AT Redstone Arsenal, AL 35898			8. PERFORMING ORGANIZATION REPORT NUMBER TR-AMR-SS-08-09	
9. SPONSORING / MONITORING AGENCY NAME(S) AND ADDRESS(ES)			10. SPONSORING / MONITORING AGENCY REPORT NUMBER	
11. SUPPLEMENTARY NOTES				
12a. DISTRIBUTION / AVAILABILITY STATEMENT Approved for public release; distribution is unlimited.			12b. DISTRIBUTION CODE A	
13. ABSTRACT (Maximum 200 Words) In order to facilitate the application of Computational Fluid Dynamics (CFD) tools by aerodynamic designers, several guidelines are developed to quantify grid generation parameters for incompressible, laminar flat plate flows. These guidelines address several factors including: (1) domain size, (2) grid point distribution functions, (3) the error to be expected from a given initial point spacing, and (4) the number of grid points (or cells) in each coordinate direction. The guidelines are discerned by comparison of computed results with the classical Blasius solution. Then they are tested and verified for a case outside the bounds of cases from which they were developed. The result is a set of "rules of thumb" that greatly simplify the grid generation process for non-specialists.				
14. SUBJECT TERMS Applied Computational Fluid Dynamics (CFD), grid generation, guidelines			15. NUMBER OF PAGES 32	
			16. PRICE CODE	
17. SECURITY CLASSIFICATION OF REPORT UNCLASSIFIED	18. SECURITY CLASSIFICATION OF THIS PAGE UNCLASSIFIED	19. SECURITY CLASSIFICATION OF ABSTRACT UNCLASSIFIED	20. LIMITATION OF ABSTRACT SAR	

NSN 7540-01-280-5500

Standard Form 298 (Rev. 2-89)
Prescribed by ANSI Std. Z39-18
298-102

ACKNOWLEDGEMENTS

This work was supported in part by a grant of High Performance Computer (HPC) time from the Engineering Research and Development Center (ERDC) and the NAVal Oceanographic (NAVO) Department of Defense (DoD) HPC centers on their Origin 2000 computational platforms.

TABLE OF CONTENTS

	<u>Page</u>
I. INTRODUCTION	1
II. METHODOLOGY	2
A. Overall Approach	2
B. Selection of Flow Solver.....	2
C. Boundary Conditions	3
D. Run Parameters	4
E. Parallelism and Modes of Communication.....	4
III. DEVELOPMENT OF GUIDELINES	5
A. Assessment of Domain Size.....	6
B. Grid Point Distribution Function	7
C. Error as a Function of Initial Grid Point Spacing.....	8
D. Number of Grid Points in Each Direction.....	11
IV. TESTING THE GUIDELINES.....	12
V. SUMMARY	15
REFERENCES	17

LIST OF ILLUSTRATIONS

<u>Figure</u>	<u>Title</u>	<u>Page</u>
1.	2.0L by 1.0L by 2.0L Computational Domain	7
2.	C_D Versus Cycle for Initial Test of Guidelines.....	9
3.	u/U_∞ Profile at $x=0.9308L$ for Initial Test of Guidelines	10
4.	v/U_∞ Profile at $x=0.9308L$ for Initial Test of Guidelines	10
5.	Local Skin Friction Coefficient Along Plate for Initial Test of Guidelines	11
6.	C_D Versus Cycle for Reference 35 Case.....	12
7.	u/U_∞ Profile at $x=5.25ft$ for Reference 35 Case	13
8.	u/U_∞ Profile at $x=5.25ft$ for Reference 35 Case After 36000 Cycles	13
9.	v/U_∞ Profile at $x=5.25ft$ for Reference 35 Case after 36000 Cycles	14
10.	Local Skin Friction Coefficient Along Plate for Reference 35 Case	14

LIST OF TABLES

<u>Table</u>	<u>Title</u>	<u>Page</u>
1.	Boundary Conditions, Run Parameters, and Communication Modes Used to Develop Guidelines	5

I. INTRODUCTION

The discipline of Computational Fluid Dynamics (CFD) has progressed to the point that both Euler and Navier-Stokes flow solvers can now be used to support the aerodynamic design process in a practical manner [1 through 7]. These solvers are generally structured, unstructured, or hybrid (that is, not “gridless”) in nature. As such, they require the creation of a solution grid on which to compute the flowfield. Hence, the construction of an appropriate grid is the key to obtaining valid results. However, this is currently an enigmatic art beyond the proficiency of most practicing aerodynamicists.

The primary difficulty in using CFD at a practical level is the uncertainty of creating an initial grid that will produce a sufficiently accurate solution for the problem at hand. Currently, one must rely on specialized expertise and experience to create an adequate initial grid. In addition, grid resolution studies, perhaps supplemented by Richardson’s extrapolation technique, must be conducted to ascertain the “goodness” of a particular grid [8 through 10]. All this must be done before further calculations can be performed with an assured level of accuracy. However, the time required to perform such “check out” computations is simply not available in a practical, fast-paced, design development or problem analysis scenario. In such an environment, quick turn-around is of paramount importance, and it is imperative that an appropriate grid be generated the first time.

Another point to consider is that the practical application of CFD to aerodynamic design is often focused only on producing adequate force and moment coefficients - products that are used in flight performance analyses, Six-Degree-of-Freedom (6-DOF) flight simulations, guidance and control system design, and High Level Architecture (HLA) simulations. In such cases, it is not necessary to determine detailed properties for the entire flowfield—only the pressure and shear forces acting directly on the body of interest. For these kinds of situations, accuracy really only needs to be maintained near the body region(s) of interest, thus relaxing any requirement for stringent precision throughout the entire solution field.

Further, the level of accuracy required exerts a strong influence on both the amount of effort spent on grid construction and the amount of Central Processing Unit (CPU) time needed for the solver to reach convergence. In other words, if engineering accuracy is satisfactory, then less-refined, “faster-running” grids can provide the desired information in a more timely and less expensive manner.

In an attempt to assist the aerodynamic designer in harnessing the powerful tool of CFD, an initial effort is made to develop some practical grid construction rules for incompressible, laminar flow over a flat plate. While this particular flow geometry has limited direct application value, it does provide a starting point for other plate-like

geometries, such as wall boundaries, airfoil surfaces, and missile fins. In addition, the guidelines developed will be soundly anchored by the Blasius solution for laminar flow over flat plates. This well-established, classical analysis provides very accurate flow data against which to test and tweak any proposed rules of thumb.

II. METHODOLOGY

A. Overall Approach

The perspective taken in this study is that of an aerodynamic designer seeking a direct, clear-cut and practical means of creating suitable CFD grids. As such, no effort is made to utilize Richardson's extrapolation technique per se in practice. While a similar approach will be used initially to develop the guidelines, the intent (in application) is to avoid the additional calculations required by this method. Rather, the idea is to quantify the expected level of accuracy a priori for simple, incompressible, flat plate flow grids.

The approach then is to first select a suitable flow solver and then determine appropriate run parameters and boundary conditions. Then the appropriate size of the computational domain will be decided and an efficacious grid point distribution function established. Afterwards, the required initial grid point (or cell size) spacing will be ascertained, and a correlation of error with initial grid point spacing will be constructed. Next the minimum number of grid points (or cells) in each coordinate direction will be investigated. The resulting guidelines will then be tested for a case outside the bounds of the cases used for their development.

B. Selection of Flow Solver

In selecting a flow solver for the conduct of this study, it should be noted that numerous valid possibilities exist. However, it should also be noted that the various solution algorithms and implementations available are likely to produce results with somewhat different accuracies for the same flow situation. Given this circumstance and a desire for the results to be generally meaningful, it becomes clear that the selected solver should be widely representative of those currently available. Further, it should be robust, computationally efficient, and easily obtainable; particularly since these criteria are likely to be key to the aerodynamic designer when selecting a practical CFD tool.

Such a tool should also be finite-volume based since such methods:

- (1) inherently conserve mass, momentum, and energy for each grid cell (versus finite difference methods which have issues maintaining conservation in three-dimensional flows),
- (2) permit the use of arbitrary, non-smooth meshes (and are thereby more general than finite-difference techniques),
- (3) adapt more naturally to zonal boundaries (and consequently handle more complex geometries than finite-difference approaches),
- (4) maintain second order accuracy at grid boundaries (versus first order for finite difference techniques), and
- (5) can handle geometries with large wall curvature and/or severely non-orthogonal grid boundaries (versus finite-difference methods which have issues with these features) [11 through 13].

A solver meeting these criteria is the Wind code [14 through 18] developed by the NPARC (National Project for Applications-oriented Research in CFD) Alliance [19]. The NPARC Alliance is a partnership between the NASA Glenn Research Center (GRC) and the Air Force Arnold Engineering Development Center (AEDC), but it also incorporates other U.S. Government, industry, and academic associates. Wind embodies the merged capabilities of the NASTD code [20 - 21] (the primary flow solver at the former McDonnell Douglas facility in St. Louis, now The Boeing Company at St. Louis), the NPARC code [22] (the original solver of the NPARC Alliance), and the NXAIR code [23 - 24] (the primary solver used at AEDC for store separation problems). As such, it is a Government-owned, three-dimensional, general-purpose flow solver for the time-dependent, compressible, Euler and Reynolds-Averaged Navier-Stokes (RANS) equations. Consequently, the use of Wind for this study should ensure the general utility of the results.

C. Boundary Conditions

To assess the appropriateness of various boundary conditions, an initial domain size had to be specified within which to perform computations. Although the required domain size will be determined later, it was crucial that the initial work be done within a sufficiently large region to avoid possible errors due to closeness of the boundaries. It was found in Hirsch [25] that a distance of 50 chords or larger between an airfoil and a boundary is not uncommon. So, a two-dimensional, rectangular domain was constructed (using Gridgen [26]) that extended 50 plate lengths above the plate and 50 lengths in both streamwise directions from the center of the plate.

In addition, a basic flow scenario had to be defined. For purposes of commonality with expected follow-on work with turbulent flow, the experimental configuration cited in Reference 27 was chosen. This configuration consisted of a large flat plate on which measurements were made in a low speed wind tunnel. The region of interest selected for the current work was the first foot of the plate, and the slowest measured velocity (58 feet-per-second) was identified as being appropriate for laminar flow. For these conditions, the boundary layer thickness was computed and used to estimate the initial grid spacing. It was presumed that 1/10 of the thickness 0.1 feet from the leading edge would provide reasonable resolution. However, in order to enable the grid to fit within the available computer memory, the initial spacing was increased by a factor of 10 to $2.5 \times 10^{-3} L$, where L = the length of the region of interest, in this case 1 foot. While such coarse resolution was inadequate to resolve the flow physics, it was felt to be sufficient to compare the relative merits of various boundary conditions.

A “Viscous Wall,” no-slip boundary condition was specified on the entire flat plate (including the part downstream of the region of interest), and an “Inviscid Wall,” slip condition was denoted on the boundary immediately upstream of the plate. These specifications remained the same throughout the duration of this investigation. However, various types of definitions were explored for the other boundaries. After numerous computations, it was discerned that using “Freestream” one-dimensional, characteristic-based conditions on the upstream and upper boundaries with “Outflow” extrapolation on

the downstream boundary worked best. The “goodness” of the calculations was assessed by comparing velocity contours throughout the field, velocity profiles near the end of the region of interest, and the skin friction distribution along the plate.

D. Run Parameters

In terms of run parameters, the previously mentioned calculations revealed the fastest, yet physically realistic, solutions were produced by the “Scalar Implicit” mode. This setting was exercised to invoke the scalar implicit form of the approximately factored implicit scheme [20] in all coordinate directions. The default would have been to apply a block implicit algorithm in the “viscous” streamwise direction. This action resulted in the viscous contributions being confined to the right-hand-side terms of the approximately factored equation – the viscous terms within the factorization were ignored. Otherwise, the default settings proved satisfactory. The other defaults: (1) implemented a second-order, upwind-biased, Roe algorithm modified for stretched grids (with a TVD [Total Variation Diminishing] minmod limiter using a limit factor of 2) for the inviscid terms, (2) employed second-order, central differencing for the viscous terms, and (3) stipulated that $CFL=1.3$.

E. Parallelism and Modes of Communication

In addition to the previous assessments, an evaluation was made of parallelism in Wind to determine an optimum number of CPUs to use. The goal was to reduce the wall clock time while maximizing CPU usage for a grid comprised of multiple zones. It was found that for an Origin 2000 computational platform, Wind 1.0 was 90 percent parallelizable [28] in the “Scalar Implicit” mode, and 98 percent parallelizable in the “Block Implicit” mode. Ten CPUs appeared to offer a “speedup” (CPU time / wall clock time) of five for scalar implicit calculations and almost nine for block implicit computations.

While these results indicated the use of 10 grid zones and 10 CPUs, they did not suggest how to structure the grid. So, an analysis was performed to learn the most effective manner to do so. After numerous variations, it was discovered that 10 vertical slices, each with 1/10 of the total grid cells, produced the best results in the shortest time. An attempt to use 10 horizontal slices simply “blew up,” perhaps due to the absence of physical boundaries in the layers above the plate. Other structures with small internal and large external zones were tried but did not work as well as the vertical slices. It turned out that using 10 vertical slices produced a better-than-expected speedup of seven over a single zone computation.

To reduce the wall clock time even further, a comparison was made between the Indirect and Direct Parallel Virtual Memory (PVM) processor communication modes that Wind uses. This was done for a 10-zone grid with 10 CPUs. It was observed that the default Indirect PVM mode only yielded a CPU to wall clock speedup of three—while the Direct PVM mode maintained the afore-mentioned speedup of seven, a decrease in wall clock time of 60 percent. Consequently, the Direct PVM mode was retained for all

subsequent computations. It should be noted, though, that according to the Wind User's Guide [29] the Direct PVM mode can only be exercised on single multi-processor systems.

At times during this effort, the Wind code was updated. When it was, a comparison was made with the previous version to ensure the codes produced identical results. Then an assessment of speedup capabilities was made and the fastest method(s) selected for use. For Wind 2.0, it was observed that only 84 percent parallelism was achievable. This was attributed to code fixes that prevented the skipping of entire Fortran DO loops. However, for Wind 3.0, the newly (at the time) implemented Message-Passing Interface (MPI) mode of communication was observed to be three times faster than Wind 2.0 with Direct PVM. Wind 3.0 with MPI also produced an additional CPU-to-wall-clock speedup of 3.4 times that of Wind 2.0 with PVM.

III. DEVELOPMENT OF GUIDELINES

A summary of the boundary conditions, run parameters, and processor communication modes used to develop the guidelines is presented in Table 1. All associated calculations were made with grids composed of 10 vertical slices using 10 CPUs as described above.

Table 1. Boundary Conditions, Run Parameters, and Communication Modes Used to Develop Guidelines

Boundary Conditions	
Location	Value
Flat Plate	Viscous Wall
Stagnation Streamline	Inviscid Wall
Upstream Boundary	Freestream
Upper Boundary	Freestream
Downstream Boundary	Outflow
Run Parameters	
Parameter	Value
Solution Methodology	Scalar Implicit
Inviscid Algorithm	2 nd Order, Upwind-Biased, Physical (stretched grid) Roe
Limiter	TVD, Minmod, Limit Factor = 2
Viscous Algorithm	2 nd Order Central
Time Step	CFL = 1.3
Processor Communication Modes	
Version of Wind	Value
Wind 1.0	PVM Direct
Wind 2.0	PVM Direct
Wind 3.0	MPI

A. Assessment of Domain Size

The assessment of domain size began by using conformal mapping to analytically estimate the appropriate location for freestream boundaries [30]. This approach succeeded in producing a relationship between influence distance and the accompanying variation of velocity from freestream conditions. For a 1 percent variation in freestream velocity, it was estimated that the grid boundaries could be located at a distance of $2.5L$ from the center of the plate.

In concert with this, a computational appraisal was conducted. This evaluation began with the “50L” grid described in the previous section. It continued by cutting the distance from the middle of the region of interest to the upstream, downstream, and upper grid boundaries by approximately half (to the closest existing grid line) each time. This was done to avoid shifting the internal grid lines and thereby make comparisons with otherwise identical grids. In the end, grids denoted as $20.7L$, $8.78L$, $3.98L$, $1.89L$, $1.0L$, $0.73L$, $0.54L$, and $0.50L$ (to designate the distance to the boundaries in terms of the length, L , of the region of interest) were examined. The results showed that the boundary distance for this incompressible case could be decreased to $1.89L$ with no detrimental effect on any of the flow variables near the body. If, however, it had been necessary to match the normal velocity component far from the plate, the boundary distance could only have been decreased to $20.7L$. In fact, the normal velocity was found to be the most sensitive indicator of parameter effects throughout the entire investigation.

To explore the previous finding further, the streamwise (x -coordinate direction) non-dimensional velocity component of the 50L grid was examined. It was scrutinized along longitudinal grid lines between the upstream boundary and the leading edge of the plate for y -coordinate locations of $10^{-6}L$, $10^{-5}L$, $10^{-4}L$, $10^{-3}L$, $10^{-2}L$, $0.1L$, L , and $10L$ units above the plate. It was noticed that the velocity component remained within 0.25 percent of the freestream value for $y \leq 0.1L$ from the upstream boundary to $x \leq -1.5L$, that is, one plate length upstream of the leading edge. This was also true for $y = 10L$. For $y = L$, however, the variation was larger, approximately 0.5 percent, at $x = -6L$. While this variation was larger and extended much further upstream, it was still less than the 1 percent variation used to analytically estimate the boundary placement.

From these results, it was concluded that: (1) the freestream boundaries for this incompressible problem could be located $2L$ units away from the center of the plate with no adverse effect, and (2) the analytical estimate provided a valid, yet conservative estimate of freestream boundary placement.

To reduce the domain size even further, the streamwise boundaries were kept at $1.89L$ while the upper boundary was located $1.89L$, $1L$, $0.5L$, $0.25L$, and $0.05L$ units above the plate. The non-dimensional streamwise velocity, u/U_∞ , was unaffected in all cases, yet the non-dimensional normal velocity, v/U_∞ , was affected by the $0.5L$ and “shorter” upper boundary placements. This consequence explains the behavior of the Wind validation calculations performed by Slater [31]. His results agreed well with the Blasius solution for u/U_∞ , but were a bit low for v/U_∞ . Examination of his upper

boundary location revealed it to be placed at $y = 0.08797L$ —well below the distance found to influence v/U_∞ .

In any case, these results made it clear that a $1.89L$ (upstream) by $1L$ (upper) by $1.89L$ (downstream) domain size would prove adequate to analyze incompressible flat plate flow. However, in order to simplify things a bit, a domain size of $2.0L$ by $1.0L$ by $2.0L$ was used for the following analyses. A sketch of this grid and the applied boundary conditions is shown in Figure 1.

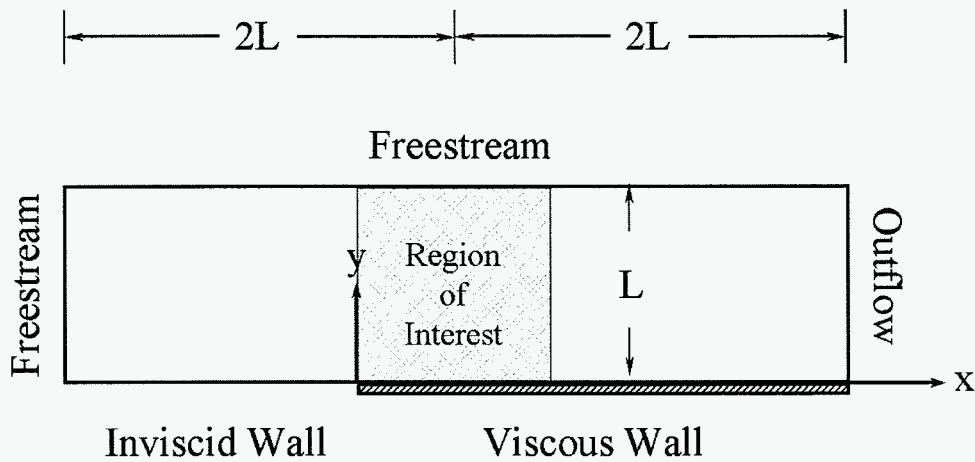


Figure 1. $2.0L$ by $1.0L$ by $2.0L$ Computational Domain

B. Grid Point Distribution Function

The most dominant attribute affecting accuracy is the spacing of grid points in the solution grid. It is for this reason that analyses and studies have been conducted to discover the relative accuracy of various grid point distribution techniques. For example, Vinokaur [32] performed a generalized truncation error analysis and found that the hyperbolic sine (\sinh) function produced the least error for one-sided point clustering, as would be typical of a wall to freestream grid. He further found that the hyperbolic tangent (\tanh) function produced the least error for two-sided clustering, as would be required for a wall-to-wall grid.

Thompson and Mastin [33] quantitatively examined the truncation error of 10 specific grid point distribution functions for scenarios of: (1) a fixed distribution function with a varying number of grid points, and (2) a fixed number of points with varying minimum point spacing. In general, they found that for a central difference discretization, the solution retained second-order accuracy regardless of the form of the point distribution function. However, only 4 of the 10 distribution functions (the exponential, hyperbolic sine, hyperbolic tangent, and error functions) were seen to produce suitable grid point spacing when the minimum spacing was small, as would be typical near a viscous wall. Their analysis further revealed the hyperbolic sine (\sinh) produced the least truncation error (of these four functions) near the wall, while away from the wall the hyperbolic tangent (\tanh) function produced less error than either the exponential (\exp) or hyperbolic sine functions. The error function (erf) was shown to behave similarly to the hyperbolic tangent function while contributing less error away from the wall. However, it was also shown to add substantially more error near the wall. To compare the two most promising distribution functions, the ratio of \sinh error to \tanh error was examined [30]. This comparison, made throughout the entire field with small values of minimum point spacing, showed that the hyperbolic tangent function provides the most accurate, general purpose distribution of grid points.

C. Error as a Function of Initial Grid Point Spacing

To perform this phase of the inquiry, the domain shown in Figure 1 was “gridded up” using an initial spacing of $0.00125L$ (half the previous value) in the upper and in both streamwise directions, centered at the leading edge. It was acknowledged that this was still too coarse to properly resolve the flow physics, but it would prove useful in comparing the relative merits of various grid cell distributions.

Computations were first made for a uniform grid. After that, they were also made for grids maintaining the same uniform streamwise spacing but exercising the \tanh point distribution function in the y -direction. These grids were constructed using the same initial point spacing with $\frac{1}{2}$, $\frac{1}{4}$, $\frac{1}{10}$, and $\frac{1}{20}$ of the number of “uniform grid” points in that direction. It was revealed that the number of points in the y -direction could be reduced to 5 percent of that required for a uniform grid with no adverse effect. Subsequent use of the \tanh function in both streamwise directions (centered at the leading edge) proved that a reduction to 50 percent of that required for a uniform grid also had no adverse effect.

At this point, the initial grid spacing was halved three successive times and the error in drag coefficient, C_D , calculated at $0.9308L$ (a point where measurements were made in Reference 27). In addition, the number of streamwise points was reduced to 25 percent and 10 percent of the uniform value. The 10 percent case was found to have only a slight effect on the v/U_∞ profile, but not C_D . At this point, it is worth noting that use of the \tanh distribution function reduced the required number of grid points substantially as compared to a uniform grid. The reduction to 10 percent and 5 percent in the streamwise and normal directions, respectively, diminished the total number to 0.5 percent of uniform number while maintaining solution accuracy.

After the previous computations were completed, the error in C_D (as compared to the Blasius value) was correlated with initial grid spacing [30]. The resulting function was used to predict the initial spacing needed to keep the error around 10 percent—an acceptable level of accuracy for many initial and intermediate design applications.

The predicted spacing was $3.36 \times 10^{-4}L$ units which was applied to the domain shown in Figure 1. The ensuing grid had 121 streamwise points upstream of the plate, 201 points along the entire length of the plate (171 of which lay in the region of interest, L), and 41 points perpendicular to the plate. This grid produced an error in C_D of only 8.85 percent, even less than the “requested” value of 10 percent. This performance demonstrated the guidelines to be capable of providing better-than-specified accuracy. Figure 2 exhibits the convergence curve, that is, coefficient versus cycle number, for C_D . Note that a cycle represents a complete iteration of the entire grid. Wind computed five iterations in each zone and then updated all zonal boundary data to complete a single cycle.

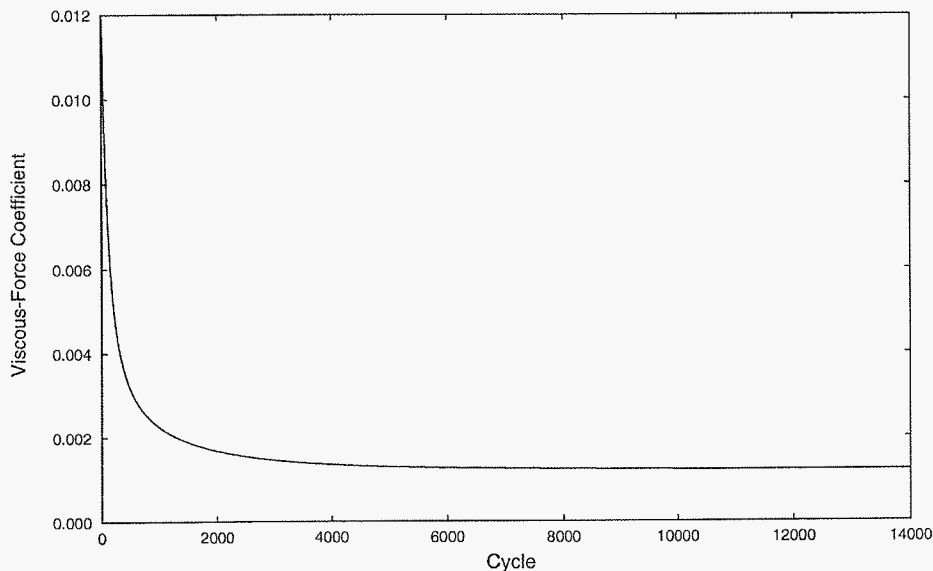


Figure 2. C_D Versus Cycle for Initial Test of Guidelines

While the guidelines performed better than expected for their intended purpose, Figures 3 through 5 show they functioned similarly well for the velocity profiles and skin friction coefficient. Figures 3 and 4 present the velocity profiles near the end of the region of interest with error bounds of ± 5 percent and ± 10 percent. It is clearly seen that the computed profile for streamwise velocity, u/U_∞ , overlays the Blasius solution while the normal velocity, v/U_∞ , is well within -5 percent of the Blasius curve. Figure 5 exhibits the computed local skin friction coefficient overlaying all but the first tenth of the Blasius values. This difference is to be expected since the grid resolution was not intended to capture the physics in this part of the field and is therefore too coarse to do so.

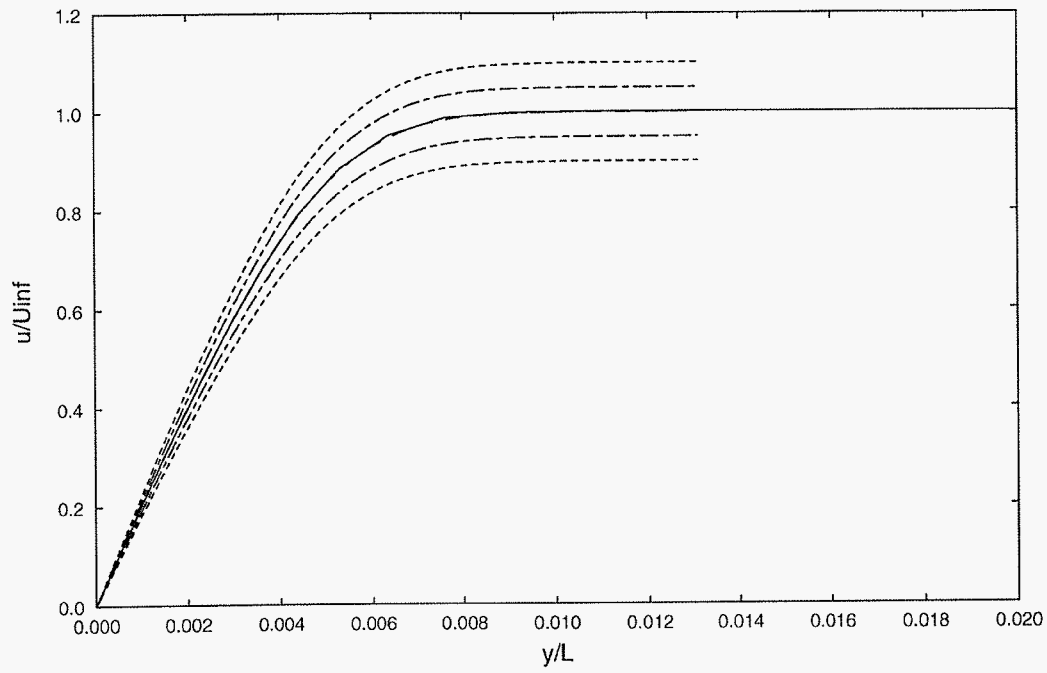


Figure 3. u/U_{∞} Profile at $x=0.9308L$ for Initial Test of Guidelines

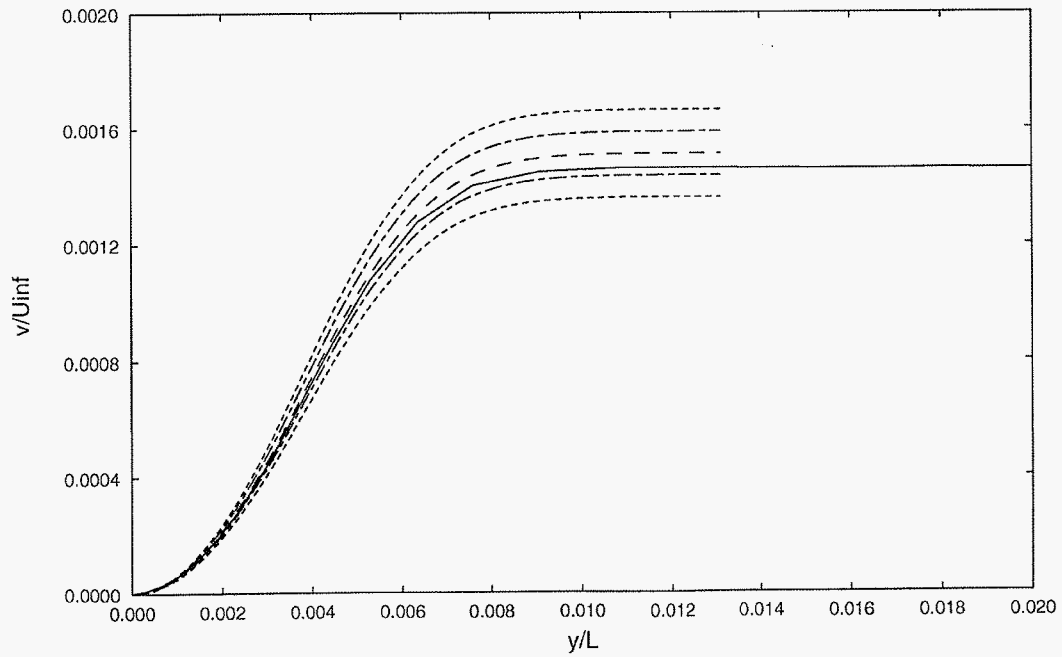


Figure 4. v/U_{∞} Profile at $x=0.9308L$ for Initial Test of Guidelines

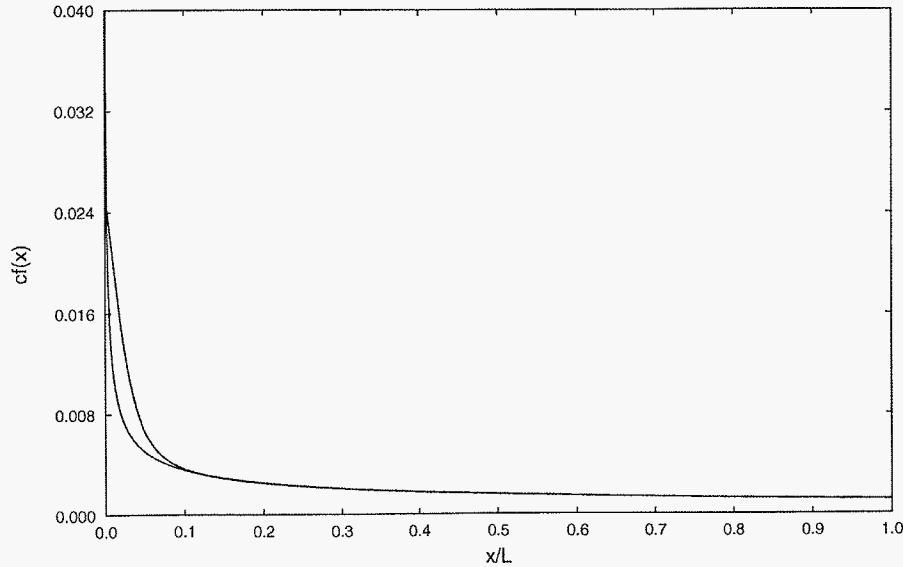


Figure 5. Local Skin Friction Coefficient Along Plate for Initial Test of Guidelines

D. Number of Grid Points in Each Direction

With the legitimacy of the guidelines established, an endeavor was made to further reduce and quantify minimum numbers of grid points needed in each coordinate direction. The previous grid was evaluated with 41, 31, 21, 16, and 11 grid points in the y-direction. It was discovered that at least 21 normal points were required to stay within an accuracy of 10 percent. This indicated the minimum required number of “y-direction” grid points to be approximately 1 percent of the number required for a uniform grid [30].

In the streamwise direction, the previous grid with 31 perpendicular and 121 upstream points was used with variations of 201, 151, 101, 51, and 26 points along the plate. This produced grids with, respectively, 171, 130, 88, 46, and 24 streamwise points in the region of interest. The downstream grid lines were allowed to vary as required by the tanh distribution function; they were not constrained at the end of the region of interest. This examination found that at least 51 streamwise points (46 in the region of interest) were needed to keep the error within 10 percent. This yielded a minimum requirement of around 2 percent of the number required to fill a uniform grid between the leading edge of the plate and the downstream boundary [30].

Continuing in this vein, the upstream region was explored using the previous grid with 151 points above the plate and 31 normal to the plate. Variations of 121, 91, 61, 31, and 16 upstream longitudinal points were inspected with little change occurring in the error for C_D . However, “kinks” occurred in the velocity profiles when less than 31 upstream points were used. Hence, a minimum requirement was determined to be about 2 percent of the number required to uniformly fill the region between the upstream boundary and the leading edge of the plate [30].

IV. TESTING THE GUIDELINES

To this point, the guidelines had only been tested for a case similar to those from which they were developed. While they performed quite well, they needed to be tested against a different laminar flat plate scenario to evaluate their generality. The instance selected was the high Reynolds number case of Schubauer and Klebanoff [34] that is presented in Reference 35. Although the flow velocity is only slightly higher, 80 feet-per-second, the measurement station of interest is located at 5.25 feet so the Reynolds number is an order of magnitude larger at 2.8×10^6 .

The grid was constructed with a 6-foot region of interest using all the previously developed guidelines. Thus, the upstream and downstream boundaries were placed 12 feet from the center of this region with the upper boundary 6 feet above the plate. The initial grid spacing was predicted to be 6.9×10^{-4} feet (for 10 percent accuracy) and the tanh function was used to distribute the points. Two hundred sixty cells (261 points) were placed in the upstream region, 440 cells (441 points) above the plate, and 87 cells (88 points) perpendicular to the plate. The results proved to be even better than expected with an accuracy in C_D of 9.6 percent at 12,000 cycles, 2.6 percent at 24,000 cycles, and 1.9 percent at 36,000 cycles. The corresponding convergence curve is shown in Figure 6.

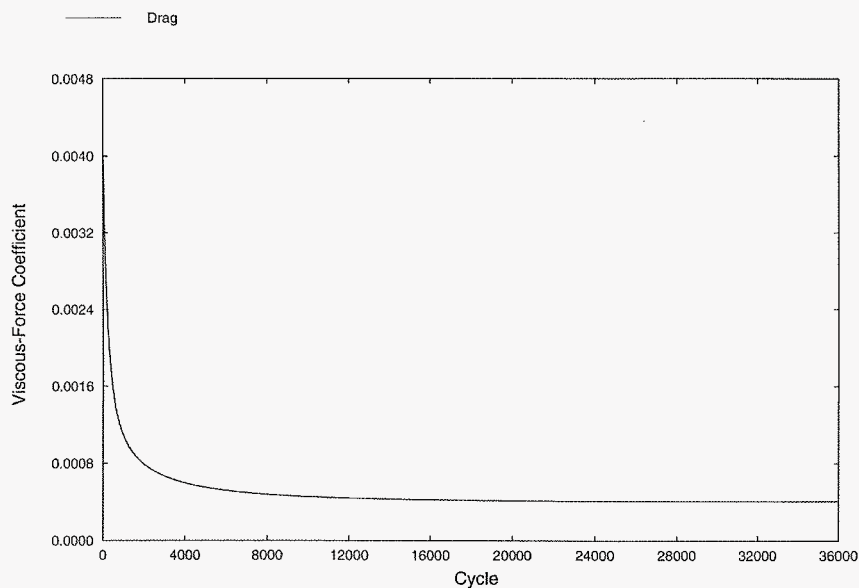


Figure 6. C_D Versus Cycle for Reference 35 Case

The results were equally good for the velocity profiles and local skin friction coefficient which are presented in Figures 7 through 10. Figure 7 illustrates the fact that even though the streamwise profile at 12,000 cycles does not overlay the Blasius solution (as the measurements and the solutions at 24,000 and 36,000 cycles do), the computed drag coefficient still has an accuracy better than the 10 percent value that was specified. Figure 8 shows that the solution at 36,000 cycles precisely overlays the Blasius curve and does not observably depart from it. Figure 9 exhibits the normal velocity at 36,000 cycles as nearly overlaying the Blasius curve and only intruding slightly into the +5 percent

region. Lastly, Figure 10 demonstrates the calculated local skin friction curves at 24,000 and 36,000 cycles also overlay the Blasius values except near the leading edge, as expected. Again, this figure underscores the point that precise capturing of the field properties is not necessary to obtain a useful force coefficient for design purposes.

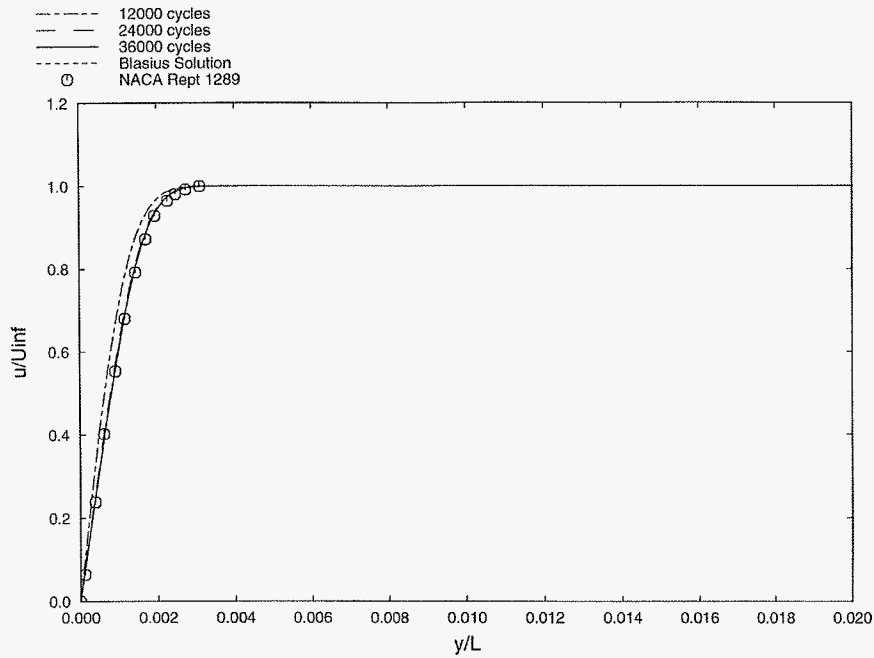


Figure 7. u/U_{∞} Profile at $x=5.25$ ft for Reference 35 Case

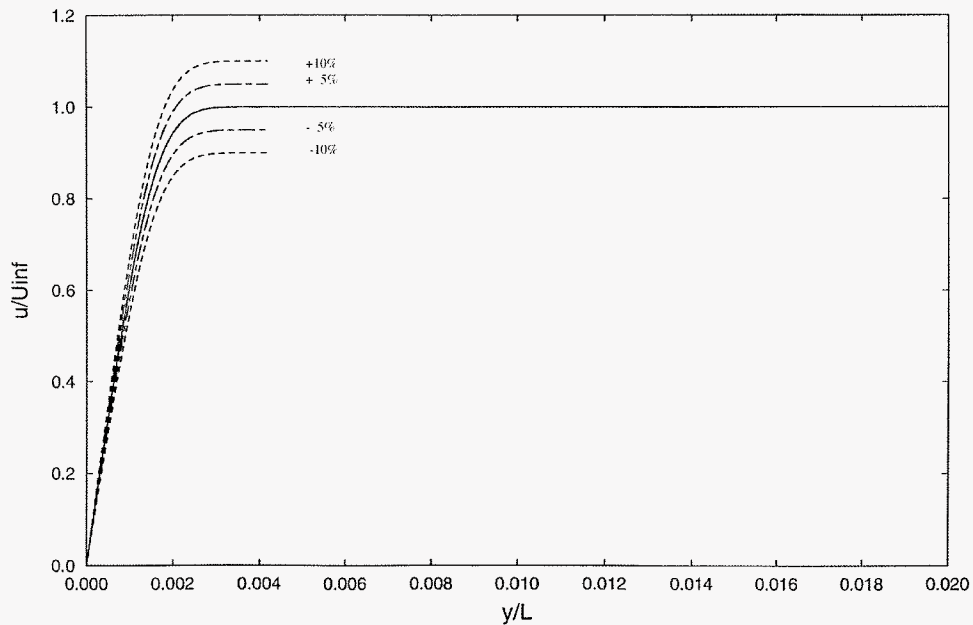


Figure 8. u/U_{∞} Profile at $x=5.25$ ft for Reference 35 Case After 36000 Cycles

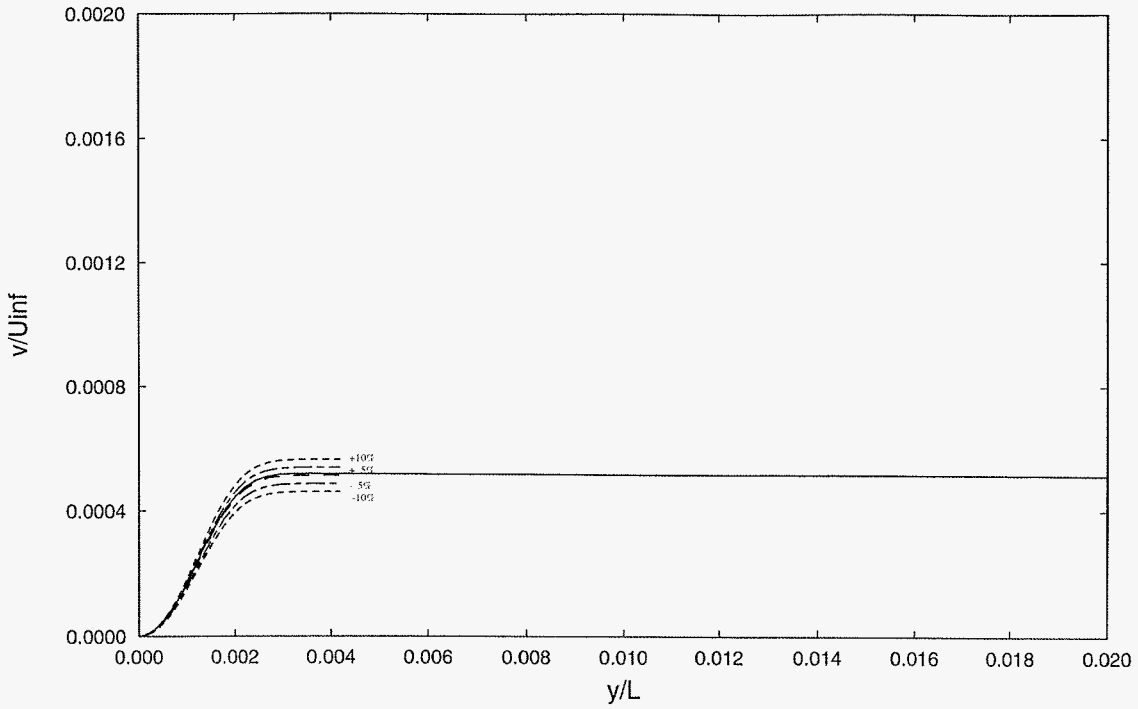


Figure 9. v/U_∞ Profile at $x=5.25\text{ft}$ for Reference 35 Case after 36000 Cycles

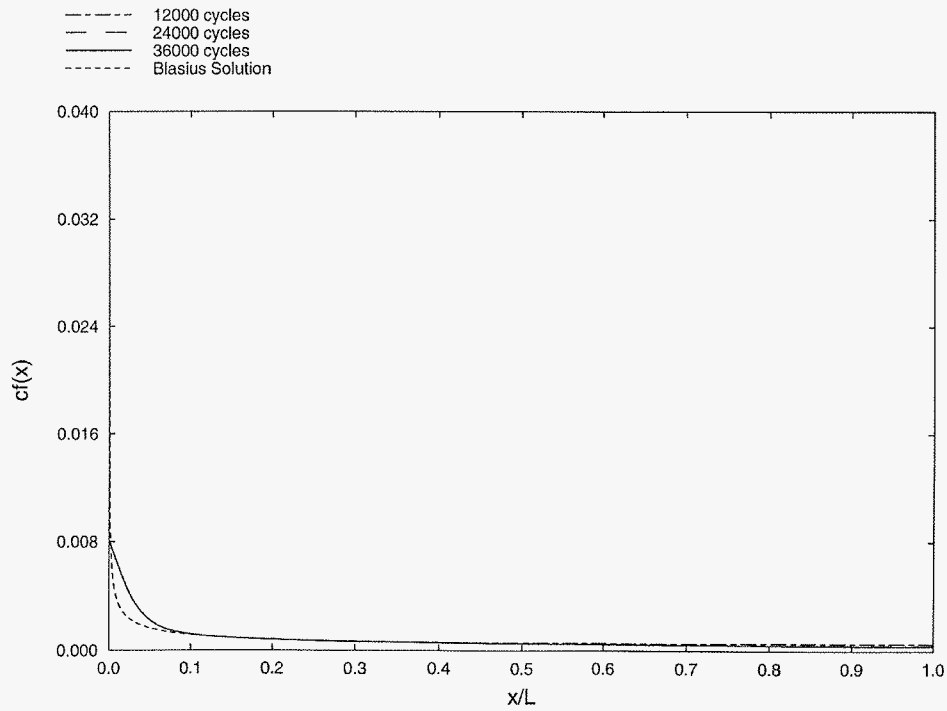


Figure 10. Local Skin Friction Coefficient Along Plate for Reference 35 Case

V. SUMMARY

The ability to predict or specify the level of accuracy for a CFD grid has been demonstrated for incompressible, laminar, flat plate flows. This is a capability that is not known to the author to have previously existed. In addition, it has been proven that the required size of the domain for incompressible flow can be predicted and is much smaller than would otherwise be expected. Further, the number of grid points required to obtain a valid solution is likewise predictable and substantially less than traditionally thought provided the hyperbolic tangent function is used to distribute them.

Although the grid generation guidelines that provide this capability were formulated for a simple type of flow, they provide a proven starting point for further development. They can also be used to provide insight into grid construction for plate-like geometries (such as flat wall boundaries, airfoil surfaces, and missile fins) in low speed flow. Moreover, they can be used directly for laminar flow problems of interest, such as flows associated with biological Micro-Electro-Mechanical Systems (MEMS) devices. In short they will, as intended, assist the aerodynamic or fluid dynamic designer in harnessing the powerful tool of CFD.

REFERENCES

1. Shivananda, T. P., Zabrensky, E. F., McKeel, S. A., and Papay, M. L., "Comparison of Engineering and CFD Predictions and Wind Tunnel Data for a Launch Vehicle Configuration," AIAA Paper 97-2251.
2. Dillenius, M. F. E., Lesieutre, D. J., Hegedus, M. C., Perkins, S. C. Jr., Love, J. F., and Lesieutre, T. O., "Engineering, Intermediate, and High Level Aerodynamic Prediction Methods and Applications," AIAA Paper 97-2278.
3. Srivastava, B., "CFD Analysis and Validation of Lateral Jet Control of a Missile," AIAA Paper 96-0288, January 1996.
4. Raj, P., "Requirements for Effective Use of CFD in Aerospace Design," Surface Modeling, Grid Generation and Related Issues in Computational Fluid Dynamics (CFD) Solutions, NASA Conference Publication 3291, May 1995, pp.15-28.
5. Srivastava, B., Furtek, J., Shelton, A., Paduano, R., "Role of CFD in Missile Aerodynamic Design: A Review of Recent Efforts at Raytheon," NATO/RTO Symposium of the Applied Vehicle Technology Panel of Missile Aerodynamics, Sorrento, Italy, May 1998, pp. 33-1 – 33-19.
6. Brédif, M., Chapin, F., Borel, C., and Simon, P., "Industrial Use of CFD for Missile Studies: New Trends at MATRA BAe DYNAMICS France," NATO/RTO Symposium of the Applied Vehicle Technology Panel of Missile Aerodynamics, Sorrento, Italy, May 1998, pp 32-1 – 32-14.
7. Vaughn, M.E., Jr. and Auman, L. M., "A Productivity-Oriented Application of Computational Fluid Dynamics to the Design of a Hypervelocity Missile," AIAA Paper 2002-2937, June 2002.
8. Roache, P. J., *Verification and Validation in Computational Science and Engineering*, Hermosa Publishers, Albuquerque, NM, 1998.
9. Celik, I., and Karatekin, O., "Numerical Experiments on Application of Richardson Extrapolation with Nonuniform Grids," *Journal of Fluids Engineering*, Vol. 119, September 1997, pp. 584 – 590.
10. Rahaim, C. P., Oberkampf, W. L., Cosner, R. R., and Dominik, D. F., "AIAA Committee on Standards for Computational Fluid Dynamics - Status and Plans," AIAA Paper 2003-0844, January 2003.
11. Vinokur, M., "An Analysis of Finite-Difference and Finite-Volume Formulations of Conservation Laws," NASA Contractor Report 177416, June 1986.

REFERENCES (CONTINUED)

12. Shu, C.-W., "High Order Finite Difference and Finite-Volume WENO Schemes and Discontinuous Galerkin Methods for CFD," NASA/CR-2001-210865, ICASE Report No. 2001-11, May 2001.
13. Schäfer, M., and Turek, S., "Benchmark Computations of Laminar Flow Around a Cylinder," http://www.featflow.de/bench_all/paper.html.
14. Bush, R. H., Power, G. D. and Towne, C. E., "Wind: The Production Flow Solver of the NPARC Alliance," AIAA Paper 98-0935, January 1998.
15. Power, G. D., and Underwood, M. L., "Wind 2.0: Progress on an Applications-Oriented CFD Code," AIAA Paper 99-3212, June/July 1999.
16. Nelson, C. C., and Power, G. D., "CHSSI Project CFD-7: The NPARC Alliance Flow Simulation System," AIAA Paper 2001-0594, January 2001.
17. Lankford, D. W., and Nelson, C. C., "Application of the Wind Flow Solver to Chemically Reacting Flows," AIAA Paper 2002-0673, January 2002.
18. Nelson, C. C., Lankford, D. W., and Nichols, R. H., "Recent Improvements to the Wind (-US) Code at AEDC," AIAA Paper 2004-0527, January 2004.
19. Matty, J., and Shin J., "The NPARC Alliance: A Progress Report," AIAA Paper 97-3353, July 1997.
20. Bush, R. H., "A Three-Dimensional Zonal Navier-Stokes Code for Subsonic Through Hypersonic Flowfields," AIAA Paper 88-2830, July 1988.
21. Mani, M., Bush, R. H., and Vogel, P. G., "Implicit Equilibrium and Finite-Rate Chemistry Models for High Speed Flow Applications," AIAA Paper 91-3299-CP.
22. Power, G. D. and Cooper, G. K., "NPARC 2.2 – Features and Capabilities," AIAA Paper 95-2609, July 1995.
23. Tramel, R. W. and Nichols, R. H., "A Highly Efficient Numerical Method for Overset-Mesh Moving-Body Problems," AIAA Paper 97-2040.
24. Nichols, R. H. and Tramel, R. W., "Applications of a Highly Efficient Numerical Method for Overset-Mesh Moving Body Problems," AIAA Paper 97-2255, June 1997.
25. Hirsch, C., Numerical Computation of Internal and External Flows, Volume 2, Computational Methods for Inviscid and Viscous Flows, John Wiley and Sons, New York, 1984, page 385.
26. <http://www.pointwise.com/gridgen>.

REFERENCES (CONCLUDED)

27. Mickley, H. S. and Davis, R. S., "Momentum Transfer for Flow Over a Flat Plate with Blowing," NACA TN 4017, November 1957.
28. Fier, J., "Performance Tuning Optimization for Origin 2000 and Onyx 2," Silicon Graphics, 1996, <http://techpubs.sgi.com>.
29. <http://www.grc.nasa.gov/WWW/winddocs/user/index.html>.
30. Vaughn, M. E., Jr., Ph.D. thesis, Department of Mechanical Engineering, University of Alabama in Huntsville, Huntsville, AL, November 2007.
31. <http://www.grc.nasa.gov/WWW/wind/valid/fplam/fplam.html>.
32. Vinokur, M., "On One-Dimensional Stretching Functions for Finite-Difference Calculations," NASA Contractor Report 3313, October 1980, also Journal of Computational Physics, Vol. 50, 1983, pp. 215-234.
33. Thompson, J. F. and Mastin, C. W., "Order of Difference Expressions in Curvilinear Coordinate Systems," Advances in Grid Generation, ASME FED - Vol. 5, 1983, pp. 17-28.
34. Schubauer, G. B. and Klebanoff, P. S., "Contributions on the Mechanics of Boundary-Layer Transition," NACA Report 1289, 1956.
35. Schlichting, H., Boundary-Layer Theory, Sixth Edition, McGraw-Hill, New York, 1968, page 435.

INITIAL DISTRIBUTION LIST

		<u>Copies</u>
Weapon Systems Technology Information Analysis Center 1901 N. Beauregard Street, Suite 400 Alexandria, VA 22311-1720	Mr. Perry Onderdonk ponderdonk@alionscience.com	Electronic
Defense Technical Information Center 8725 John J. Kingman Rd., Suite 0944 Fort Belvoir, VA 22060-6218	Jack Rike jriike@dtic.mil	Electronic
AMSRD-AMR		Electronic
AMSRD-AMR-CS-IC		Electronic
AMSRD-AMR-SS,	Mr. Gregory B. Tackett Gregory.Tackett@us.army.mil	Electronic
AMSRD-AMR-SS-AT,	Mr. Lamar M. Auman lamar.auman@us.army.mil Mr. Milton E. Vaughn, Jr. Ed.Vaughn@us.army.mil	Electronic Electronic
AMSRD-L-G-I,	Ms. Anne Lanteigne anne.lanteigne@us.army.mil	Electronic